



Numerical Study on the Ultimate Bearing Capacity of the Strip Foundations on the Inclined Multi-Layered Soil Mass with a Weak Layer

Majid Kianpour¹ · Ahad Bagherzadeh Khalkhali² · Rouzbeh Dabiri³ · Mehdi Mahdavi Adeli⁴

Received: 16 July 2023 / Accepted: 1 January 2024 / Published online: 21 March 2024
© The Author(s), under exclusive licence to Shiraz University 2024

Abstract

Engineers frequently encounter challenges in designing foundations located above buried structures. In order to examine the effect of partial loading on the bearing capacity of inclined strip foundations situated within weak soil layers, small-scale model tests are conducted. Although thin layers may appear insignificant, they have a considerable influence on the ultimate bearing capacity. To investigate this phenomenon, a series of laboratory model tests were conducted on rigid strip footings positioned on various stratified embankment foundation surfaces. The experimental procedure encompasses different foundation configurations, incorporating variations in material type, thickness, and slope of the thin layers. The results obtained from the laboratory analysis indicate that the eccentricity value significantly affects the bearing capacity of the foundation. Additionally, the bearing capacity is observed to increase as the foundation moves away from the weak layer and the edge of the slope. Notably, the presence of a weak layer at the critical distance of $B=0$ results in an additional 43% reduction in the bearing capacity (from 23.75 to 34.07 kPa).

Keywords Weak thin layer · Inclined multi-layer soil · Ultimate bearing capacity · Eccentricity · Numerical model

Abbreviations

B	Footing width, foundation distance from slope edge
e	Eccentricity without tension under foundation
e'	Eccentricity in the test
q	Bearing capacity
c'	Cohesion
C_c	Coefficient of curvature

C_u	Uniformity coefficient
D_{\max}	Maximum grain size
D_r	Relative density
D_f	Embedment depth of foundation
D_{10}	Effective grain size
D_{30}	Diameter corresponding to 30%
D_{50}	Average grain size
D_{60}	Diameter corresponding to 60% finer
G_s	Specific gravity
N_p, N_q	Bearing capacity factors
q	Bearing pressure
q_u	Ultimate bearing capacity of uniform sand with thin layer
q_{u0}	Ultimate bearing capacity of uniform sand
S	Settlement of the foundation
R	Footing radius
t_i	Thickness of thin layer
Z_i	Depth from the ground surface of thin layer
γ	Unit weight
γ_d	Dry unit weight
$\gamma_{d\max}$	Maximum dry unit weight
$\gamma_{d\min}$	Minimum dry unit weight
φ'	Angle of internal friction
σ_n	Normal stress

✉ Ahad Bagherzadeh Khalkhali
a-bagherzadeh@srbiau.ac.ir
Majid Kianpour
Majid.kianpour@srbiau.ac.ir
Rouzbeh Dabiri
rouzbeh_dabiri@iaut.ac.ir

¹ Civil Engineering Faculty, Islamic Azad University Science and Research University, Tehran, Iran
² Civil Engineering Faculty, Science and Research Branch, Islamic Azad University, Tehran, Iran
³ Department of Civil Engineering, Tabriz Branch, Islamic Azad University, Tabriz, Iran
⁴ Department of Civil Engineering, Shoushtar Branch, Islamic Azad University, Shoushtar, Iran

σ_v	Vertical stress
$\Delta q/\Delta s$	Variation of bearing pressure to variation of settlement ratio

1 Introduction

The ultimate bearing capacity of foundations is a critical aspect of geotechnical engineering design. Various theories and methods have been developed to accurately determine the bearing capacity of foundations, including limit equilibrium theory, slip line theory, limit analysis theory, and others (Terzaghi 1943; Meyerhof 1951; Hansen 1970; Chen 1975; Michalowski 1997; Soubra 1999; Wang et al. 2001).

The classical bearing capacity equation, initially proposed by Terzaghi (1943) based on the Mohr–Coulomb equation, considers soil cohesion, foundation loading, and unit weight of soil. However, in practical applications, foundations may experience combined loads, including vertical, horizontal, and eccentric loads resulting from wind and wave forces, as well as the self-weight of the superstructure. To address these scenarios, capacity factors for eccentric and oblique loads proposed by Meyerhof (1953, 1963), Hansen (1970), and Vesic (1975) are commonly utilized. Furthermore, tilting loads on the ultimate bearing capacity are typically accounted for through semi-empirical correction factors (Terzaghi 1943).

Numerical methods, such as finite element analysis, have been employed to solve the capacity solution of strip foundations under various loading conditions. Taiebat and Carter (2002) used the finite element method to determine the capacity solution of a strip foundation under eccentric loading on pure undrained soil. Loukidis et al. (Hjiaj et al. 2004) investigated the load-carrying capacity of strip foundations under eccentric and oblique loading, considering non-associated flow degrees. Additionally, Zheng et al. (2019) studied the bearing capacity of sandy soil strip foundations on clay soils under oblique loads using a discontinuous layout optimization method.

The combination of limit analysis theory and finite element techniques has been employed to examine the ultimate bearing capacity of foundations under oblique loads. Researchers such as Hjiaj et al. (2004); Loukidis et al. (2008); and Krabbenhoft, Damkilde, and Krabbenhoft (2014) applied finite element analysis in conjunction with limit analysis theory to assess the bearing capacity of foundations under eccentric and oblique loads on different soil types.

The research has addressed this issue in conduit foundations under practical conditions.

2 Methodology

The objective of this research is to investigate the effect of variations in slope mass angle, loading eccentricity, and weak layer location on the bearing capacity of foundations subjected to loads on sandy soils with laboratory physical modeling and numerical simulation, simultaneously. Reaching this goal, a series of finite element analyzes were conducted using the numerical software Geo-Studio (2013). The slope angle and eccentricity were systematically varied to encompass a wide range of practical scenarios. Then, the resulting failure envelope shapes were compared to the experimental data from the physical models conducted in the laboratory.

Consideration of minor geological details, such as slip surfaces, shear bands, and thin layers, is essential as they significantly influence the behavior of soil–foundation systems (Valor et al. 2017). The presence of a weak layer in a sand bed has been found to significantly affect the ultimate bearing capacity of strip foundations (Heroic et al. 2017). Settlement of layered soil is also crucial for the seismic bearing capacity of strip foundations (Money et al. 2015; Qin and Chian 2018; Xiao et al. 2019; Wu et al. 2019; Veiskarami et al. 2017).

Despite the considerable research on bearing capacity, relatively few studies have assessed the load–settlement response and bearing capacity of footings placed over buried conduits while considering the variation in soil density (Terzi 2007). Srivastava et al. (2013) conducted plate load tests to investigate the effect of soil density on the carrying capacity of a circular footing over a buried conduit. Bildik and Laman (2015, 2019) examined the bearing capacity of strip footings assuming the ground to be at an infinite level, but limited research has addressed this issue in conduit foundations under practical conditions (Keshavarz et al. 2017).

2.1 Analytical Model

Numerical simulations were conducted based on a scaled-down physical model. In this analysis, load capacity factors were determined from the load–displacement curve. To replicate the actual experimental procedure and account for the high stiffness of the foundation and roughness of its base (Lee et al., 2013), a uniform vertical settlement of the foundation base was assumed.

The numerical analysis involved determining load capacity factors based on the variable parameters of the test program. Various methods are available for numerical analysis, including finite difference, finite element method, boundary elements, and discrete elements. In this study,

the behavior of the stratified soil was modeled using linear and nonlinear soil models found in geotechnical application software packages such as PLAXIS, GEO-STUDIO, FLAC, and ABAQUS.

An extensive finite element analysis was conducted using the Geo-Studio 2D software package. By validating the numerical model against laboratory results, the need for experimentation under various conditions can be reduced, resulting in a return on investment. Geo-Studio 2D is a two-dimensional finite element software package commonly used for static and dynamic analysis of soil and rock, and it was utilized in this study. The software allows for the visualization of load-settlement diagrams and determination of the bearing capacity of foundations and circular piles. Furthermore, the software's capability for axisymmetric modeling enables the creation of circular foundations.

The finite element software Geo-Studio was employed to create the model and perform the calculations. The area of interest was discretized into multiple elements in SIGMA/W. In this case, the unknown stresses vary linearly within each element. Figure 1 provides an illustration of the finite element mesh, which was generated using Geo-Studio software.

Figure 1 also depicts a numerical model of a rigid strip foundation resting on a rock mass under plane strain conditions in SIGMA/W. The foundation and rock mass are assumed weightless and represented by rigid plate elements and solid elements, respectively. The interface between the plates and rocks is treated as rough. Fan meshes were implemented at the foundation corners to obtain more accurate solutions for the lower boundaries.

2.2 Laboratory Physical Modeling

To investigate the distribution characteristics of deformations, stresses, and failure zones of a sand foundation and determine its bearing capacity, a physical model test was conducted using a shallow strip footing. The schematic representation of the strip foundation is shown in Fig. 2. This

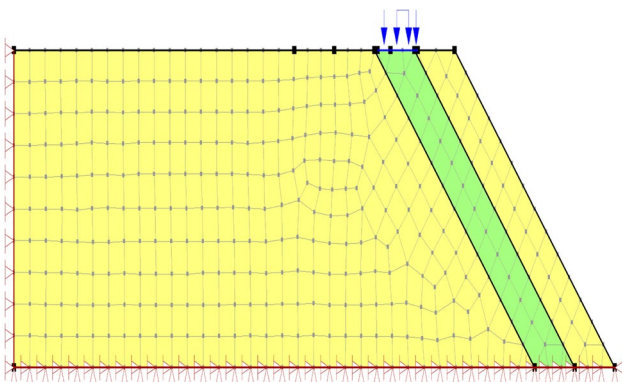


Fig. 1 Finite element meshing

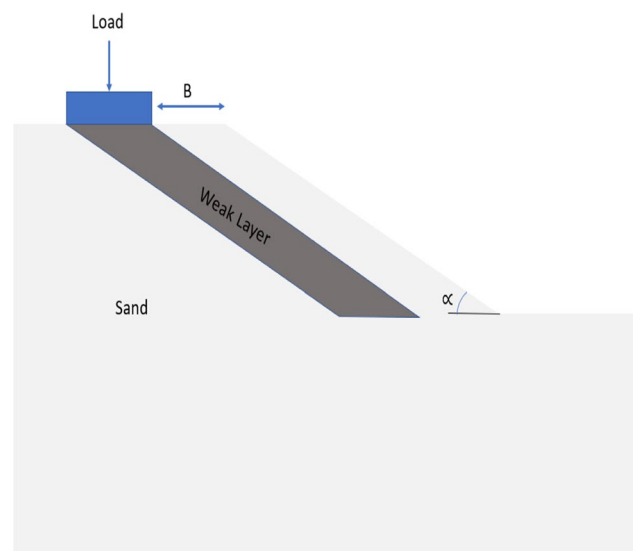


Fig. 2 Scheme of the experiment model

foundation was studied under uniaxial conditions, making it like a rigid strip foundation. The strip foundation is positioned on a steep slope within the soil mass, with an initial depth of zero. Figure 2 presents a typical schematic representation of the foundation model on a sand bed. The study focused on variations in soil type, thickness, and slope of the weak layer. Crushed silica sand with medium density (SP) was used as the bed sand in this study. To facilitate the required tests and verify changes in bearing capacity, a small-scale experimental model was designed and constructed, as shown in Fig. 1.

The test box features a hydraulic jack located on top, which applies static loads to both the foundation and the soil contained within as shown in Fig. 3. The tank walls are reinforced with horizontal and vertical stiffeners to prevent lateral deformation. A portion of the tank's side walls is made of 20 mm thick glass, allowing for observation of the soil beneath the foundation. The inner walls of the tank are smoothly polished. All tests were performed with the soil under the foundation at ground surface level. A rigid frame was employed to transfer vertical loads to the foundation.

The variable parameters of the experiment, denoted as e , B , and α , are illustrated in Fig. 2. In this diagram, e represents the load eccentricity, B indicates the distance of the weak layer from the inclined edge, and α denotes the angle of inclination of the sand mass.

To test the bearing capacity of the soil mass, the physical model and laboratory prototype were developed in different phases, following a step-by-step approach. To prevent the test box walls from influencing the results, the initial step involved setting the net internal dimensions of the test box to 150 cm (length), 60 cm (width), and 50 cm (height). The model's strip foundation is a rigid metal piece measuring

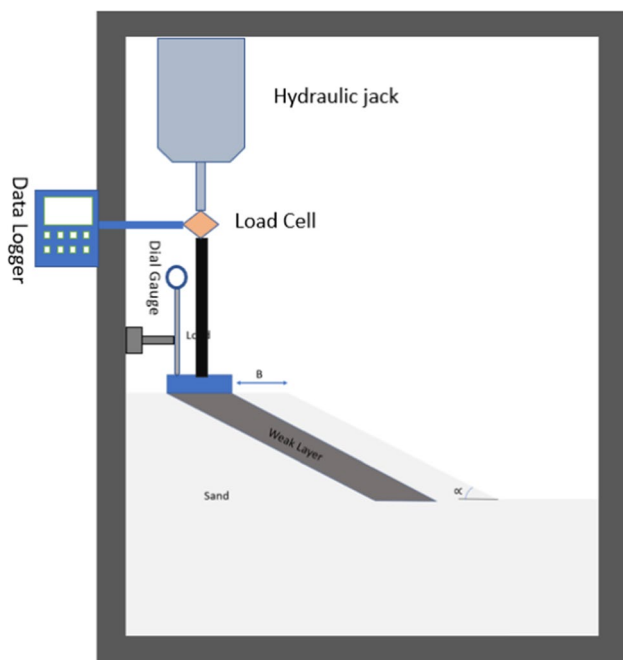


Fig. 3 Section view of the physical model

60 cm in length and 5 cm in width. Subsequently, the embankment was backfilled in layers, with each layer of soil poured into the box at a thickness of 5 cm and compacted to achieve the desired relative density. These steps were repeated until reaching the desired height level beneath the foundation.

2.3 Specifications and Operation of the Test Box

As mentioned previously, the designed physical model consists of a rectangular steel tank with dimensions of 1 m in length, 0.7 m in width, and 0.7 m in depth. The bearing capacity tests were conducted using a steel foundation measuring 8.0 cm in width, 70.0 cm in length, and 3.5 cm in thickness. The problem was studied under axisymmetric conditions. The required density of the sand was achieved using the sand precipitation (rainfall) method.

2.4 Specifications and Operation of the Test Box

As mentioned previously, the designed physical model consists of a rectangular steel tank with dimensions of 1 m in length, 0.7 m in width, and 0.7 m in depth. The bearing capacity tests were conducted using a steel foundation measuring 8.0 cm in width, 70.0 cm in length, and 3.5 cm in thickness. The problem was studied under axisymmetric conditions. The required density of the sand was achieved using the sand precipitation (rainfall) method.

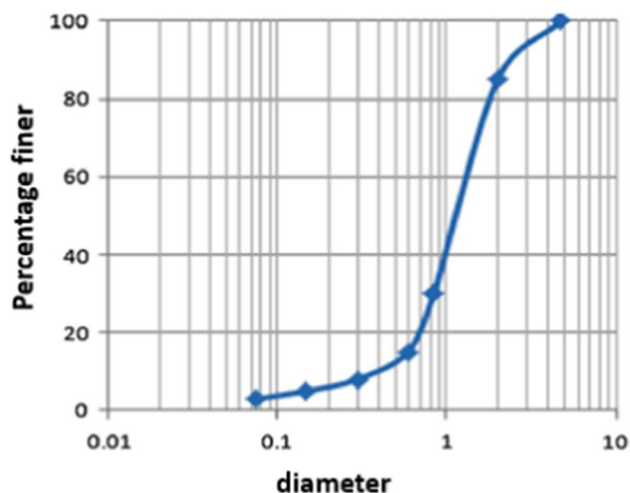


Fig. 4 Particle-size distribution curve for sand

Loading simulations were performed by applying pressure to the strip foundation. The applied pressure was transmitted to the foundation through a hydraulic jack with a constant displacement speed of 1 mm/min. The load applied by the hydraulic cylinder was recorded by a load cell mounted on the cylinder shaft. Settlements generated in the soil mass were measured using a high-precision plate gauge with a measurement accuracy of at least 0.01 mm. It should be noted that using a manual hydraulic jack to apply the load may result in slight changes in the loading rate. However, under static load conditions, the loading rate's effect on settlement and bearing capacity of the surface foundation is insignificant (Bildik and Laman 2015). A data acquisition system comprising a data logger and computer software was employed to extract load and displacement data for analysis.

3 Material features

The study involved two types of soil: clay and sand, classified as CL and SP, respectively, according to the Unified Soil Classification System. The moisture content of the soil layers was maintained below 2% during the experiments, with the aid of plastic sheet isolators.

Sand properties

The sand used in the physical model was obtained from the Quartz Sand Factory on Firouzkoh Street. The sand was used under dry weather conditions. According to the Unified Soil Classification System (USCS), the sand is described as poorly classified sand (SP). Figure 4 illustrates the grading curve of the silica sand utilized in the study. To achieve a uniform relative density in the tests, the sand was poured from the same drop height using the dry rain method. The box was emptied and refilled for each experiment. Some

Table 1 Properties of the sand used in the model tests

Properties	Value	Standard No
shear strength	1	ASTM
Maximum grain size, D_{max} (mm)	2.38	ASTM D C136
Diameter corresponding to 60% finer, D_{60} (mm)	1.45	
Average grain size, D_{50} (mm)	1.20	
Diameter corresponding to 30% 30%, D_{30} (mm)	0.9	
Effective grain size, D_{10} (mm)	0.61	
Uniformity coefficient, C_u	2.16	
Coefficient of curvature, C_c	0.83	
Specific gravity, G_s	2.66	ASTM D 854
Maximum dry unit weight, γ_{dmax} (kN/m ³)	19.85	ASTM D 4254
Minimum dry unit weight, γ_{dmin} (kN/m ³)	13.73	ASTM D 4253
Dry unit weight, γ_d (kN/m ³)	15.71	
Relative density, D_r (%)	41	
Classification (USCS)	SP	ASTM D 2487

physical properties of the sand are listed in Table 1. The relative density, D_r , was determined in accordance with ASTM D 4253 and D 4253 standards. The effects of particle size were considered negligible since the ratio B/d_{50} exceeded 50 (Bolton and Love (1989); Taylor (1995) and Toyosawa et al. (2013)). Additionally, the shear strength parameters of the Firozkoh sand used in the soil mass were determined through seven direct shear tests, following ASTM D 3080.

Weak layer properties

The weak layer on the embankment comprised materials with lower shear strength compared to the sand bed. Compressible clay powder classified as CL was used to create the weak layer, with a natural moisture content of 5.5% in all tests. Table 2 presents some technical properties of the thin weak layer. Due to the low moisture content of the clay soil, no pore pressure was generated during the tests, and thus, no additional pore pressure was considered. The shear strength properties of the clay were also determined through seven direct shear tests, following the standard procedures. The results indicated that the shear strength characteristics of the

Table 2 Physical properties of weak layer used in the model tests

Property	Value	Standard No
Specific gravity, G_s	2.68	ASTM D854
Unit weight, γ (kN/m ³)	12.1	ASTM D6683
Liquid limit (%)	26	ASTM D4318
Plastic limit (%)	18	
Plasticity index (%)	8.0	
Classification (USCS)	CL	ASTM D2487
Water content (%)	5.5	ASTM D2216

thin weak layer material were not significantly influenced by the stress level and loading is controlled by displacement.

4 Experimental Procedure

At the beginning of the experiment, the sand rain guard was placed directly above the sandbox. Subsequently, sand was applied in 5 cm thick layers using the precipitation method. During the sand rainfall, the density of the sand was controlled by placing cans with a specific volume at different locations within the box. Simple molds were used to create a sand slope with a specific angle at the desired depth, thickness, and weak layer. Additional layers of sand were poured until reaching the desired surface, after which the foundation model was placed at a specified point on the sand bed's surface. Finally, vertical pressure was applied to the foundation model using a manual hydraulic cylinder at a constant speed of 1 mm per minute.

A numerical measuring device with an accuracy of 0.01 mm was used to measure the vertical settlement of the soil mass. In some cases, tests were repeated to ensure a certain level of confidence in the results. The capacity results for each type of test were reviewed for different variables of the physical model.

The variable parameters used in the experiments, as shown in Table 1, along with their values, are listed in Table 3. The experiments were divided into two series: the behavior of the foundation on a uniform sandy slope base, the behavior of the foundation on the sandy slope bed with a weak layer at different thicknesses, depths, and angles.

4.1 Experiment Programs

Using the created physical model, approximately 20 load-bearing tests were conducted, considering various values of the variables defined in the article. The schedule of the physical tests corresponding to the variables is presented in Table 3.

In accordance with the information provided in Table 3, a comprehensive set of experiments was carried out to explore the behavior of the foundation under various conditions. Initially, the focus was on investigating the response of the foundation situated on a uniformly composed sandy

Table 3 Model test program

Type of test	Constant parameters	Variable parameters
Uniform sand	$D_r = 41\%$, $D_f = 0$	–
Uniform sand with weak layer	$D_r = 41\%$, $D_f = 0$	$B' = 0, 0.5b, b$ $e' = e/3, e/2, e/4$ $\alpha = 30, 45, 60$

embankment base. Subsequently, attention shifted toward analyzing the behavior of the foundation on a sandy slope bed incorporating a weak layer. Finally, the influence of variable values, including the distance from the toe of the slope and the slope angle, on the foundation's behavior was examined.

5 Results and Discussion

The pressure-settlement curves of the foundations were derived from the experimental results of the test model, along with the outcomes of the numerical analysis conducted in this phase. These curves were subsequently compared to the corresponding experimental data. Notably, the settlement of the foundation (S) was expressed in dimensionless terms, specifically as a ratio ($S/B, \%$), where S represents the settlement and B denotes the foundation width.

5.1 Experimental Results

The initial phase of the investigation involved analyzing the behavior of a strip foundation positioned on a uniform sand slope. Based on the pressure-settlement curve obtained from the results, the ultimate bearing capacity was determined to be 37.6 kPa. The corresponding settlement value at the peak was found to be 26 mm, with a relative settlement ($S/B, \%$) of 32.5%.

Next, pressure-settlement curves were generated for strip footings resting on a sandy embankment base incorporating a weak layer with a thickness of $T = 50$ mm. The experiments were conducted by varying the values of the variable parameters, and the resulting pressure-settlement outcomes are depicted in Fig. 5. The findings demonstrate that the presence of the weak thin layer leads to a reduction in both the bearing capacity and stiffness of the soil-foundation system.

Furthermore, the study examined the effect of the inclination angle on the obtained results. It was observed that as the inclination angle increases, the determined bearing capacity decreases. The critical value of the inclination angle (α) was identified as 45 degrees, which serves as the threshold for further testing procedures.

The experimental investigations conducted under various conditions have provided valuable insights into the behavior of strip foundations in the presence of a weak layer and varying distances from the slope edge. The results indicate a noticeable decrease in the bearing capacity of the strip footing when a weak layer is introduced, underscoring the detrimental effect of its presence on the overall load-bearing capacity. Furthermore, it is observed that an increase in the distance (B) between the strip foundation and the slope edge leads to an augmented bearing capacity. Specifically, the experiments reveal a significant 43% increase in the

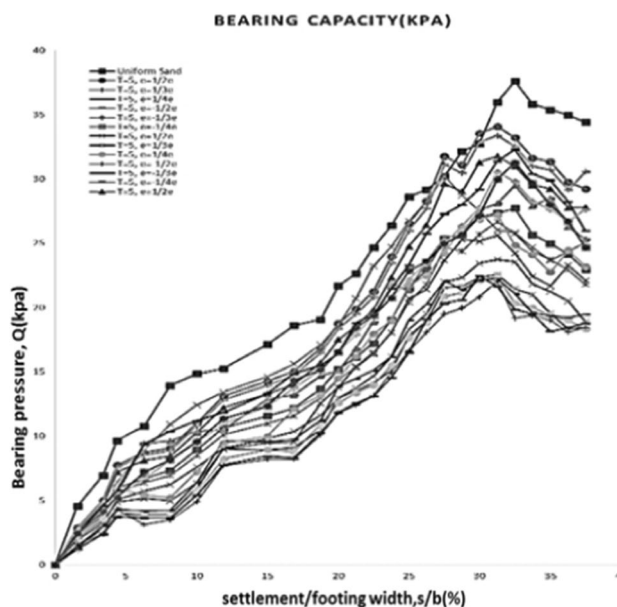


Fig. 5 Pressure-settlement curve of strip footing on sand with a weak layer for all value of B

bearing capacity, ranging from 23.75 to 34.07 kPa, as the B parameter is increased. These findings are further supported by the trends observed in Fig. 5, which clearly demonstrate that higher values of B and eccentricity result in an enhanced bearing capacity relative to the slope edge. A comprehensive overview of the bearing capacity data for all tested scenarios is provided in Table 4, presenting a comprehensive summary of the experimental results.

5.2 Numerical Results

To complement the experimental findings, an extensive finite element analysis was conducted using the Geo-Studio software package. By employing a two-dimensional finite element model, the software enabled a comprehensive examination of soil mass loading and deformation behavior. This numerical modeling approach, validated and calibrated using laboratory results, serves as a valuable tool in reducing the need for extensive experimental testing under different conditions.

Sigma/W module within the Geo-Studio software facilitated the visualization of load-settlement diagrams and determination of the maximum stress-induced allowable deformation, which correlates with the ultimate bearing capacity. The shear strength parameters obtained from direct shear tests, as presented in Table 1 and 2, were utilized in defining the properties of the clay and sandy soils within the numerical models. A total of 19 numerical models were constructed in accordance with the specifications outlined in Table 3 to obtain the desired results.

Table 4 Ultimate bearing capacity of all type of tests

Test No	Test data	Ultimate bearing capacity Qu (KPa)
1	T=0, e' =0, B=0, D=15	37.587
2	T=5, e' = 1/2e, B=0	23.750
3	T=5, e' = 1/3e, B=0	22.560
4	T=5, e' = 1/4e, B=0	22.410
5	T=5, e' = -1/2e, B=0	22.040
6	T=5, e' = -1/3e, B=0	22.246
7	T=5, e' = -1/4e, B=0	22.459
8	T=5, e' = 1/2e, B=0.5b	31.789
9	T=5, e' = 1/3e, B=0.5b	30.223
10	T=5, e' = 1/4e, B=0.5b	27.771
11	T=5, e' = -1/2e, B=0.5b	25.620
12	T=5, e' = -1/3e, B=0.5b	26.685
13	T=5, e' = -1/4e, B=0.5b	27.235
14	T=5, e' = 1/2e, B=b	34.071
15	T=5, e' = 1/3e, B=b	33.378
16	T=5, e' = 1/4e, B=b	32.292
17	T=5, e' = -1/2e, B=b	29.500
18	T=5, e' = -1/3e, B=b	30.558
19	T=5, e' = -1/4e, B=b	31.250

Table 5 Ultimate bearing capacity for strip footings with weak layer (Numerical results)

Test data	Q _{ult} (KPa) Numerical output
No 1	33.6
No 2	26.19
No 3	25.67
No 4	24.92
No 5	24.15
No 6	23.78
No 7	23.56
No 8	29.49
No 9	28.9
No 10	27.21
No 11	26.44
No 12	26.14
No 13	25.86
No 14	30.24
No 15	29.78
No 16	29.28
No 17	28.66
No 18	28.85
No 19	29.57

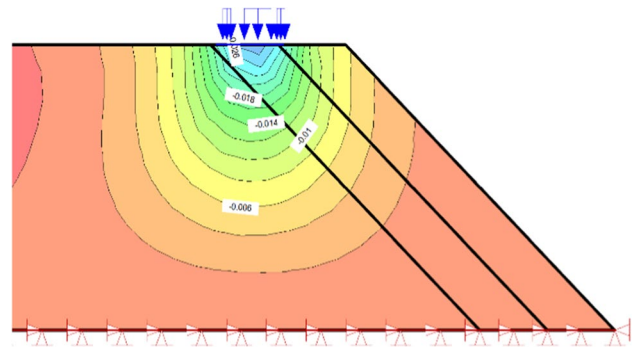


Fig. 6 Vertical displacement distribution result of strip footing Test No. 14 (Allowable settlement)

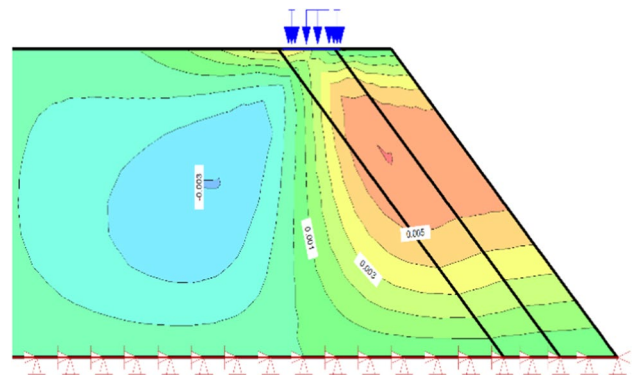


Fig. 7 Horizontal displacement distribution result of strip footing Test No. 14

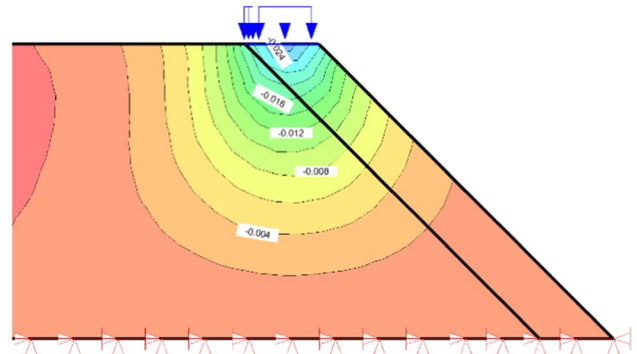


Fig. 8 Vertical displacement distribution result of strip footing Test No. 2 (Allowable settlement)

Table 5 presents the numerical analysis results for strip footings on soils both with and without a weak layer, providing a comprehensive overview of the outcomes obtained from the numerical simulations. Additionally, Figs. 6 illustrate the load-settlement diagrams for strip footings with and without a weak layer. The comparison between the numerical results presented in Table 5 and the corresponding

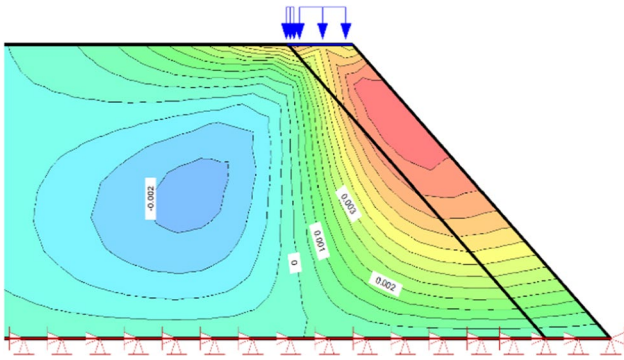


Fig. 9 Horizontal displacement distribution result of strip footing Test No. 14

experimental evidence demonstrates the significant influence of weak clay layer thickness and depth on the bearing capacity of the layered soil. Figures 7, 8, 9 illustrate the displacement behavior of strip footings for Experiment No. 14 and No. 2, respectively.

The results reveal that the magnitude of overburden and the position of the weak layer exert a substantial influence on the ultimate bearing capacity of the foundation. For instance, within the scope of this study, the maximum bearing capacity exhibited an 11% reduction compared to Test No. 1, while the worst-case scenario within the test program displayed a significant 42% decrease in the bearing capacity of the strip foundation.

In general, the findings demonstrate that, akin to the uniform sand case, different tests were conducted for various values of the weak layer parameters, with corresponding numerical analysis employed to model these scenarios. As demonstrated in Table 5, the test group featuring a larger distance (B) compared to other values of the B parameter exhibited the highest bearing capacity values. Conversely, a decrease in this value, resulting in the weak layer being situated closer to the top of the slope, led to a reduction in the bearing capacity.

6 Conclusion

In this study, the behavior of strip foundations on sandy slopes with and without weak layers was thoroughly investigated through a combination of experimental and numerical analysis. The following key findings were obtained:

6.1 Behavior of Strip Foundation on Uniform Sandy Slope

The ultimate bearing capacity of the strip foundation on a uniform sand slope was determined to be 37.6 kPa.

The settlement corresponding to the peak bearing capacity was found to be 26 mm.

The relative settlement ($S/B, \%$) was calculated as 32.5%, with settlement presented dimensionless in relation to the foundation width (B).

6.2 Effect of Weak Layer on Bearing Capacity

The addition of a weak layer to the sandy embankment base significantly reduced both the bearing capacity and stiffness of the soil–foundation system.

The thickness of the weak layer was found to have a significant effect on the bearing capacity of the layered soil.

6.3 Influence of Distance from Slope Edge (B)

The weak thin layer for the critical distance of $B=0$ led to more reduction in the ultimate bearing capacity by 43% (from 23.75 to 34.07 kPa). The closest values of bearing capacity to the uniform sand state occurs when $B=B$. The lowest bearing capacity also occurs when $B=0$.

6.4 Comparison between Experimental and Numerical Results

The numerical analysis using the Geo-Studio software package provided valuable insights into the behavior of the soil–foundation system.

The results obtained from the numerical models were in good agreement with the experimental evidence, validating the reliability of the numerical approach.

The numerical analysis demonstrated that the size of the overburden and the location of the weak layer significantly influenced the ultimate bearing capacity of the foundation.

Overall, this study highlights the importance of considering weak layers and the distance from the slope edge when designing strip foundations on sandy slopes. The findings emphasize the need for careful evaluation and consideration of these factors to ensure the stability and optimal performance of such foundations in practical engineering applications.

It is worth noting that further research and analysis may be required to explore additional parameters and variables that could affect the behavior of strip foundations on sandy slopes.

6.5 Carrying Capacity Check

The presence of a weak layer reduces the bearing capacity of the foundation.

The hardness of the soil-foundation system. The extent of this effect.

It depends on the thickness and depth of the weak layer.

The existence of a strong layer has increased the carrying capacity of the foundation and the hardness of the soil-foundation system. The extent of this effect.

It depends on the thickness and depth of the strong layer.

Another goal of this research is that the geotechnical engineer.

During field research, you should never skimp on the details.

Small geological like thin layers remain oblivious.

No funding was received to assist with the preparation of this manuscript.

References

- MF Bildik M Laman 2015 Bearing capacity of strip footings on non-homogeneous slopes Int J Geotech Eng 9 3 252 261 <https://doi.org/10.1179/1939787914Y.0000000054>
- MF Bildik M Laman 2019 Ultimate bearing capacity of strip footing on non-homogeneous slopes J Civ Eng Manag 25 4 369 380 <https://doi.org/10.3846/jcem.2019.9764>
- ZY Chen 1975 Load capacity of strip foundations on clay J Geotech Geoenvironmental Eng 101 6 513 526 [https://doi.org/10.1061/\(ASCE\)0733-9410\(1975\)101:6\(513\)](https://doi.org/10.1061/(ASCE)0733-9410(1975)101:6(513))
- JB Hansen 1970 A revised and extended formula for bearing capacity Dan Geotech Inst Bull 11 2 12 23
- AG Heroic 2017 Failure mechanism and ultimate bearing capacity of strip foundation on a sand bed with a weak layer Geotech Eng J SEAGS & AGSSEA 48 3 61 67 <https://doi.org/10.13140/RG.2.2.17608.01284>
- M Hjjaj AV Lyamin SW Sloan 2004 Lower bound limit analysis of strip footings on non-homogeneous soils Géotechnique 54 3 167 174 <https://doi.org/10.1680/geot.2004.54.3.167>
- D Loukidis T Chakraborty R Salgado 2008 Bearing capacity of strip foundations under eccentric and oblique loading: a numerical study Int J Geomech 8 5 277 286 [https://doi.org/10.1061/\(ASCE\)1532-3641\(2008\)8:5\(277\)](https://doi.org/10.1061/(ASCE)1532-3641(2008)8:5(277))
- GG Meyerhof 1951 The ultimate bearing capacity of foundations Géotechnique 2 4 301 331 <https://doi.org/10.1680/geot.1951.2.4.301>
- RL Michalowski 1997 Evaluating bearing capacity factors for eccentrically loaded foundations J Geotech Geoenvironmental Eng 123 10 941 951 [https://doi.org/10.1061/\(ASCE\)1090-0241\(1997\)123:10\(941\)](https://doi.org/10.1061/(ASCE)1090-0241(1997)123:10(941))
- ME Money 2015 Seismic slope stability of layered soil deposits: A numerical study Soil Dyn Earthq Eng 74 120 128 <https://doi.org/10.1016/j.soildyn.2015.03.009>
- Y Qin SC Chian 2018 Seismic behavior of two-story slopes with layered soil deposits Soil Dyn Earthq Eng 104 61 70 <https://doi.org/10.1016/j.soildyn.2017.11.007>
- AH Soubra 1999 Bearing capacity under eccentric and inclined loads J Geotech Geoenvironmental Eng 125 10 823 831 [https://doi.org/10.1061/\(ASCE\)1090-0241\(1999\)125:10\(823\)](https://doi.org/10.1061/(ASCE)1090-0241(1999)125:10(823))
- A Srivastava 2013 Plate load tests on buried conduit J Geotech Geoenvironmental Eng 139 9 1509 1513 [https://doi.org/10.1061/\(ASCE\)GT.1943-5606.0000913](https://doi.org/10.1061/(ASCE)GT.1943-5606.0000913)
- K Terzaghi 1943 Theoretical Soil Mechanics Wiley
- Y Terzi 2007 Load-settlement response of footings on sands overlying clays Can Geotech J 44 6 640 652 <https://doi.org/10.1139/T06-131>
- M Veiskarami R JamshidiChenari AA Jameei 2017 Bearing capacity of strip footings on anisotropic soils by the finite elements and linear programming Int. J. Geomech. ASCE 17 12 04017119 [https://doi.org/10.1061/\(ASCE\)GM.1943-5622.0001018](https://doi.org/10.1061/(ASCE)GM.1943-5622.0001018)
- AS Vesic 1975 Analysis of ultimate loads of shallow foundations J Geotech Eng Div 101 4 359 378

Springer Nature or its licensor (e.g. a society or other partner) holds exclusive rights to this article under a publishing agreement with the author(s) or other rightsholder(s); author self-archiving of the accepted manuscript version of this article is solely governed by the terms of such publishing agreement and applicable law.